AD_____

Award Number: W81XWH-11-1-0372

TITLE: Intracellular Protein Delivery for Treating Breast Cancer

PRINCIPAL INVESTIGATOR: Pin Wang

CONTRACTING ORGANIZATION: University of Southern California
Los Angeles, CA 90089-0701

REPORT DATE: June 2013

TYPE OF REPORT: Annual Report

PREPARED FOR: U.S. Army Medical Research and Materiel Command
Fort Detrick, Maryland 21702-5012

# REPORT DOCUMENTATION PAGE

*Form Approved*
*OMB No. 0704-0188*



| 1. REPORT DATE | 2. REPORT TYPE | 3. DATES COVERED |
|---|---|---|
| June 2013 | Annual | 15 May 2012 to 14 May 2013 |

**4. TITLE AND SUBTITLE**
Intracellular Protein Delivery for treating Breast Cancer

**5a. CONTRACT NUMBER**

**5b. GRANT NUMBER**
W81XWH-11-1-0372

**5c. PROGRAM ELEMENT NUMBER**

**6. AUTHOR(S)**
Pin Wang

E-Mail: yitang@ucla.edu

**5d. PROJECT NUMBER**

**5e. TASK NUMBER**

**5f. WORK UNIT NUMBER**

**7. PERFORMING ORGANIZATION NAME(S) AND ADDRESS(ES)**
University of Southern California
Los Angeles, CA 90089-0701

**8. PERFORMING ORGANIZATION REPORT NUMBER**

**9. SPONSORING / MONITORING AGENCY NAME(S) AND ADDRESS(ES)**
U.S. Army Medical Research and Materiel Command
Fort Detrick, Maryland 21702-5012

**10. SPONSOR/MONITOR'S ACRONYM(S)**

**11. SPONSOR/MONITOR'S REPORT NUMBER(S)**

**12. DISTRIBUTION / AVAILABILITY STATEMENT**
Approved for Public Release; Distribution Unlimited

**13. SUPPLEMENTARY NOTES**

**14. ABSTRACT**

Apoptin-containing nanocapsules have been shown to be efficiently internalized by mammalian cells and induce tumor-specific apoptosis in vitro and in vivo. Identification of targeting moieties can further improve the efficacy of these nanopartciles. Targeting nanoparticles by conjugating various specific ligands has shown potential therapeutic efficacy in nanomedicine. However, poor penetration of antitumor drugs into solid tumors remains a major obstacle. We demonstrated a targeting strategy by conjugating nanoparticles with a tumor-penetrating peptide, iRGD. The results showed that iRGD could facilate the binding and cellular uptake of nanoparticles. Colocalization data revealed that iRGD-conjugated nanoparticles entered cells via the clathrin-mediated pathway, followed by endosome-lysosome transport. In addition, we were able to demonstrate that the biofunctional chelator AmBaSar could be used in the $^{64}$Cu labeling of nanoparticles and the positron emission tomography-based images of particle distribution could be obtained at several time points after intravenous administration of nanoparticles. Our data support the further experiment to use iRGD for targeting nanocapsules and to use PET imaging for investigating bioditribution of nanocapsule in vivo.

**15. SUBJECT TERMS**
Nanogels, core-shell, redox-responsive, apoptosis, breast cancer.

| 16. SECURITY CLASSIFICATION OF: | | | 17. LIMITATION OF ABSTRACT | 18. NUMBER OF PAGES | 19a. NAME OF RESPONSIBLE PERSON |
|---|---|---|---|---|---|
| a. REPORT | b. ABSTRACT | c. THIS PAGE | | | 19b. TELEPHONE NUMBER *(include area code)* |
| U | U | U | UU | 11 | USAMRMC |

## Table of Contents

## INTRODUCTION

Specific induction of cell death in tumors is considered one of the most desired and effective anticancer therapies. Effective strategies to activate the apoptotic pathway, or other death mechanisms, are currently being intensely pursued. A potent chemotherapy option is directly arming the cancer cells with executioner proteins or apoptotic-inducing proteins that are not targeted by anti-apoptotic maneuvers found in many tumors. In this proposal, we will develop a new method to treat breast cancer by using a native-protein delivery approach. This is a platform to deliver proteins in native forms into cells. The key design feature of our strategy is to first encapsulate protein molecules in a thin layer of water soluble, positively charged, degradable polymer to form nanometer-sized nanocapsules. The nanocapsule shell facilitates uptake of the protein content into cells, and protects the protein both during in vivo circulation and endocytosis. To endow the nanocapsules biodegradability once entered the target cells, the polymer shell is crosslinked with redox-sensitive crosslinkers that can be reduced upon encountering the reducing environment of the cytoplasm. Our overall research objective is to thoroughly evaluate this delivery method as a potentially new therapeutic modality for breast cancer treatment. Three aims will be pursued in parallel and results from each aim will be used to guide the refinement of other aims and the overall research objective. 1) Delivering different target proteins to breast cancer cell lines using this approach, including the tumor specific apoptin; 2) Equipping the protein nanocapsules with specific cancer cell targeting ligands; 3) Examining the in vivo potency and pharmacokinetics of the nanocapsules.

## BODY

### Summary of State of Work

**Specific Aim 1: Delivering different target proteins to breast cancer cell lines using protein nanocapsules**

Task 1. Preparing and characterizing of Apoptin contained nanocapsules
This task has been completed in the first year. Detailed description can be found in the first year's report.

Task 2. *in vitro* studying Apoptin contained nanocapsules
This task has been completed in the first year. Detailed description can be found in the first year's report.

**Specific Aim 2: Equipping protein nanocapsules with specific cancer cell targeting ligands;**

Task 3. Preparing and testing of MMP activatable cell penetrating peptides (ACCPs)-coupled nanocapsules
This task is currently under evaluation, no results to report at this point.

Task 4. Preparing and testing of ligand-receptor affinity based targeting: Transferrin (Tf) and Herceptin
This task has been partially performed and some results will be in the following pages.

**Specific Aim 3: Examining the *in vivo* potency and pharmacokinetics of the nanocapsules.**

Task 5. Evaluating *in vivo* distribution of protein nanocapsules
This task has been partially performed and some results will be in the following pages.

Task 6. Examining the *in vivo* pharmacokinetics of nanocapsules
This task has been partially performed and some results will be in the following pages.

Task 7. Determing the *in vivo* delivery efficacy of nanocapsules
This task has been completed. Detailed description can be found in the first year's report

## Background and Motivation

**Intracelluar delivery of recombinant proteins for cancer therapy** The most desirable cancer therapy is both potent and specific towards tumor cells (Gibbs 2000; Atkins and Gershell 2002). Many conventional small molecule chemotheraputics do not discriminate between cancerous and normal cells, cause undesirable damage to healthy tissues, and are therefore unable to be administered at high dosage. In contrast, cytoplasmic and nuclear proteins that selectively alter the signaling pathways in tumor cells, reactivate apoptosis and restore tissue homeostasis, can eradicate cancerous cells and delay tumor progression with less collateral damage to other tissues (Evan and Vousden 2001; Reed 2003; Cotter 2009). Intracellular delivery of such proteins, including human tumor suppressors (such as p53) (Brown, Lain et al. 2009) and exogenous tumor-killing proteins (such as apoptin) (Backendorf, Visser et al. 2008), in their functional forms is attractive as a new anti-cancer therapy modality.

**Apoptin** Apoptin is a small protein (121 amino acids) from chicken anemia virus (CAV) that induces p53-independent apoptosis in a tumor-specific way (Backendorf, Visser et al. 2008). In a variety of tumor cell lines, Apoptin becomes phosphorylated, enters the nucleus, and induces apoptosis (Zhuang, Shvarts et al. 1995; Danen-Van Oorschot, Fischer et al. 1997; Danen-Van Oorschot, Zhang et al. 2003). In sharp contrast, Apoptin is unphosphorylated in normal cells and stays in the cytoplasm. An important feature of Apoptin is that it can recognize early stages of oncogenesis and it can induce apoptosis. Currently known Apoptin targets include DEDAF, Nur77, Nmi, and Hippi, some of which are p53-independent signaling proteins in the apoptotic pathway (Backendorf, Visser et al. 2008). Due to its high selectivity and potency, Apoptin has become an attractive antitumor target for gene therapy approaches. For example, in a nude mouse model, injection of Apoptin-encoding adenoviruses to the site of breast carcinoma xenografts resulted in a significant reduction in tumor growth. Furthermore, Apoptin has been shown to be a safe agent, resulting in minimal toxicity and weight loss in mouse models. Recombinant Apoptin expressed by *E. coli* can induce rapid apoptosis in cancer cells when microinjected into tumor cells (Leliveld, Zhang et al. 2003). In comparison, no apoptosis was observed in normal cells. Moreover, when fused to the HIV-TAT protein transduction domain, TAT-Apoptin was transduced efficiently into normal and tumor cells. However, TAT-Apoptin remained in the cytoplasm and did not kill normal 6689 and 1BR3 fibroblasts. In contrast, TAT-Apoptin migrated from the cytoplasm to the nucleus of Saos-2 and HSC-3 cancer cells resulting in apoptosis after 24 h (Guelen, Paterson et al. 2004). These results indicate that recombinant Apoptin captures all of the essential functions and selectivity of the native protein. Therefore, Apoptin is an excellent target for expanding the applications of nanocapsules as a chemotherapy modality.

### Task 4: Preparing and testing of ligand-receptor affinity based targeting: Transferrin (Tf) and Herceptin

As we are working on the design of targeting strategies for nanocapsules, new progress has emerged from the field. As we all know that one of major obstacle for nanoparticle-based drug delivery is the poor penetration of the targeted payload through the vascular wall and into the tumor parenchyma, especially in solid tumors, which have a high interstitial pressure (Heldin et al., 2004; Jain, 1999). To address this challenge, a tumor-penetrating peptide, iRGD, was identified and reported to increase vascular and tissue penetration in a tumor-specific and neuropilin-1-dependent manner, as compared to the conventional RGD peptides (Sugahara et al., 2009; Sugahara et al., 2010). Like conventional RGD peptides, iRGD homes to tumor sites by binding to $\alpha_v\beta_3$ and $\alpha_v\beta_5$ integrins, which are highly expressed in tumor endothelium (Mitra, Mulhollan et al. 2005; Murphy, Majeti et al. 2008; Sugahara, Teesalu et al. 2009), thus enhancing the therapeutic effect of antitumor drugs on suppressing tumor growth and/or metastasis. After binding, the iRGD peptide is thought to be proteolytically cleaved to produce CRGDK fragment, which favors binding to neuropilin-1 receptor, thus facilitating the penetration of drugs into the tumor (Feron 2010). Thus, we explored whether the iRGD peptide could improve the nanoparticle delivery. As a proof of concept, our work initially focused on the crosslinked multilamellar liposomal vesicle (cMLV)-based nanoparticles as a model system to test the assays and biological efficacy, which can be directly translated into nanocapsules.

**Synthesis of iRGD-conjugated nanoparticles** Preparation of liposomes was based on the conventional dehydration-rehydration method. All lipids were obtained from NOF Corporation (Japan). 1.5 μmol of lipids 1,2-dioleoyl-sn-glycero-3-phosphocholine (DOPC), 1,2-dioleoyl-sn-glycero-3-phospho-(1'-rac-glycerol) (DOPG), and maleimide-headgroup lipid 1,2-dioleoyl-sn-glycero-3-phosphoeth-anolamine-N-[4-(p-maleimidophenyl) butyramide (MPB-PE) were mixed in chloroform to form a lipid composition with a molar ratio of DOPC:DOPG:MPB = 4:1:5, and the organic solvent in the lipid mixture was evaporated under argon gas, followed by additional drying under vacuum overnight to form dried thin lipid films. The resultant dried film was hydrated in 10 mM Bis-Tris propane at pH 7.0 with doxorubicin at a molar ratio of 0.2:1 (drugs:lipids) with vigorous vortexing every 10 min for 1 h and then applied with 4 cycles of 15-s sonication (Misonix Microson XL2000, Farmingdale, NY) on ice at 1 min intervals for each cycle. To induce divalent-triggered vesicle fusion, $MgCl_2$ was added to make a final concentration of 10 mM. The resulting multilamellar vesicles were further crosslinked by addition of dithiothreitol (DTT, Sigma-Aldrich) at a final concentration of 1.5 mM for 1 h at 37°C. The resulting vesicles were collected by centrifugation at 14,000 g for 4 min and then washed twice with PBS. For iRGD conjugation to cMLVs, the particles were incubated with 0.5 μmol of iRGD peptides (GenScript, Piscataway, NJ) for 1 h at 37°C. For pegylation of cMLVs, both unconjugated and iRGD-conjugated particles were further incubated with 0.5 μmol of 2 kDa PEG-SH (Laysan Bio Inc., Arab, AL) for 1 h at 37°C. The particles were then centrifuged and washed twice with PBS. The final products were stored in PBS at 4°C. The hydrodynamic size and size distribution of iRGD-NPs were measured by dynamic light scattering (Wyatt Technology, Santa Barbara, CA). The hydrodynamic size of these targeted nanoparticles was measured by dynamic light scattering (DLS), and the result showed the mean diameter of iRGD-NPs to be ~230 ± 11.23 nm, which was similar to that of unconjugated cMLV (~220 ± 6.98 nm).

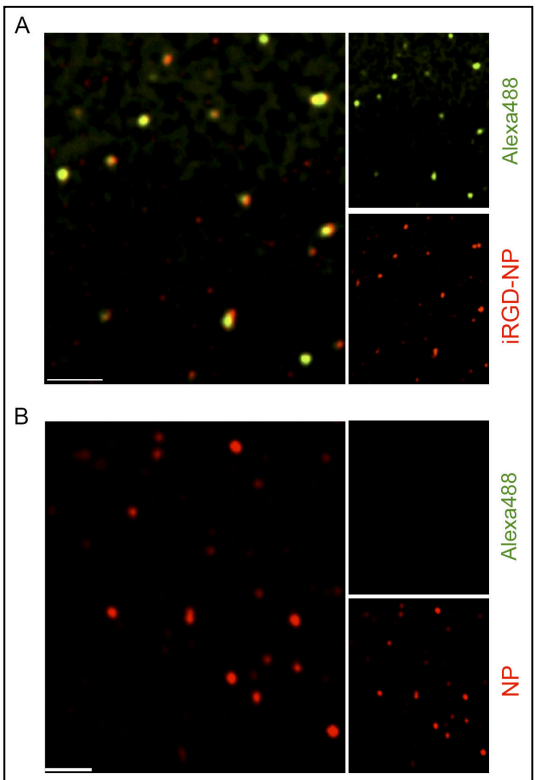


Figure 1: Conformation of the conjugation of iRGD peptides onto the nanoparticles by confocal imaging. DiD-labeled iRGD-NPs (A) and DiD-labeled NPs (B) were reacted with Alexa488 dye for 1 h at room temperature followed by confocal imaging. Scale bar represents 5μm.

To examine whether iRGD peptides were conjugated to the surface of nanoparticles via the maleimide headgroups, fluorescent 1,1-dioctadecyl-3,3,3,3-tetramethylindodicarbocyanine (DiD)-labeled nanoparticles were used to visualize both unconjugated and conjugated particles. In addition, Alexa488 dye was utilized to label iRGD peptides through the amine group of lysine residues on iRGD peptides (CRGD**K**GPDC). The results showed that a significant colocalization of DiD-labeled iRGD-NPs with Alexa488-labeled iRGD peptides was observed (Figure 1A), while no Alexa488 signals were detected on unconjugated particles (Figure 1B), suggesting that iRGD peptides were successfully conjugated to nanoparticles.

**Internalization and intracellular pathways of iRGD-cMLVs** We next investigated the entry mechanism and intracellular process of iRGD-NPs into tumor cells to determine whether iRGD peptides could change the pathway by which nanoparticles are endocytosed. Endocytosis is known as one of the main entry mechanisms for various nanoscale drug carriers (Dobson and Kell 2008; Petros and DeSimone 2010). Several studies have reported the involvement of clathrin- and caveolin-dependent pathways in nanoparticle-mediated endocytosis (Pelkmans and Helenius 2002; Conner and Schmid 2003; Le Roy and Wrana 2005). Therefore, to investigate the role of clathrin- or caveolin-dependent endocytosis of iRGD-NPs, we visualized the individual fluorescent DiD-labeled NPs or iRGD-NPs with endocytic structures (clathrin or caveolin) after 15 min incubation at 37°C. As shown in Figure 2A, a significant colocalization of unconjugated nanoparticles with caveolin-1 signals was observed, while no colocalization between unconjugated nanoparticles and clathrin structures was detected, indicating that the caveolin pathway may be involved in the endocytosis. However, after 15 min incubation, iRGD-NPs were colocalized with clathrin structures, whereas, no significant colocalization between iRGD-NPs and caveolin-1 signals was observed (Figure 2B), suggesting that the endocytosis of iRGD-NPs could be clathrin-dependent. The quantification of iRGD-NPs and NPs colocalized with caveolin-1 or clathrin structures by analyzing more than 30 cells confirmed that the clathrin-mediated pathway could be involved in the entry of

iRGD-NPs, while the endocytosis of NPs could be caveolin-1-dependent (Figure 2C and 2D). The role of clathrin-dependent endocytosis of iRGD-NPs was further examined by drug-inhibition assays shown in Figure 2E. Chlorpromazine (CPZ) is known to block clathrin-mediated internalization by inhibiting clathrin polymerization (Wang, Rothberg et al. 1993), while filipin is a cholesterol-binding reagent that can disrupt

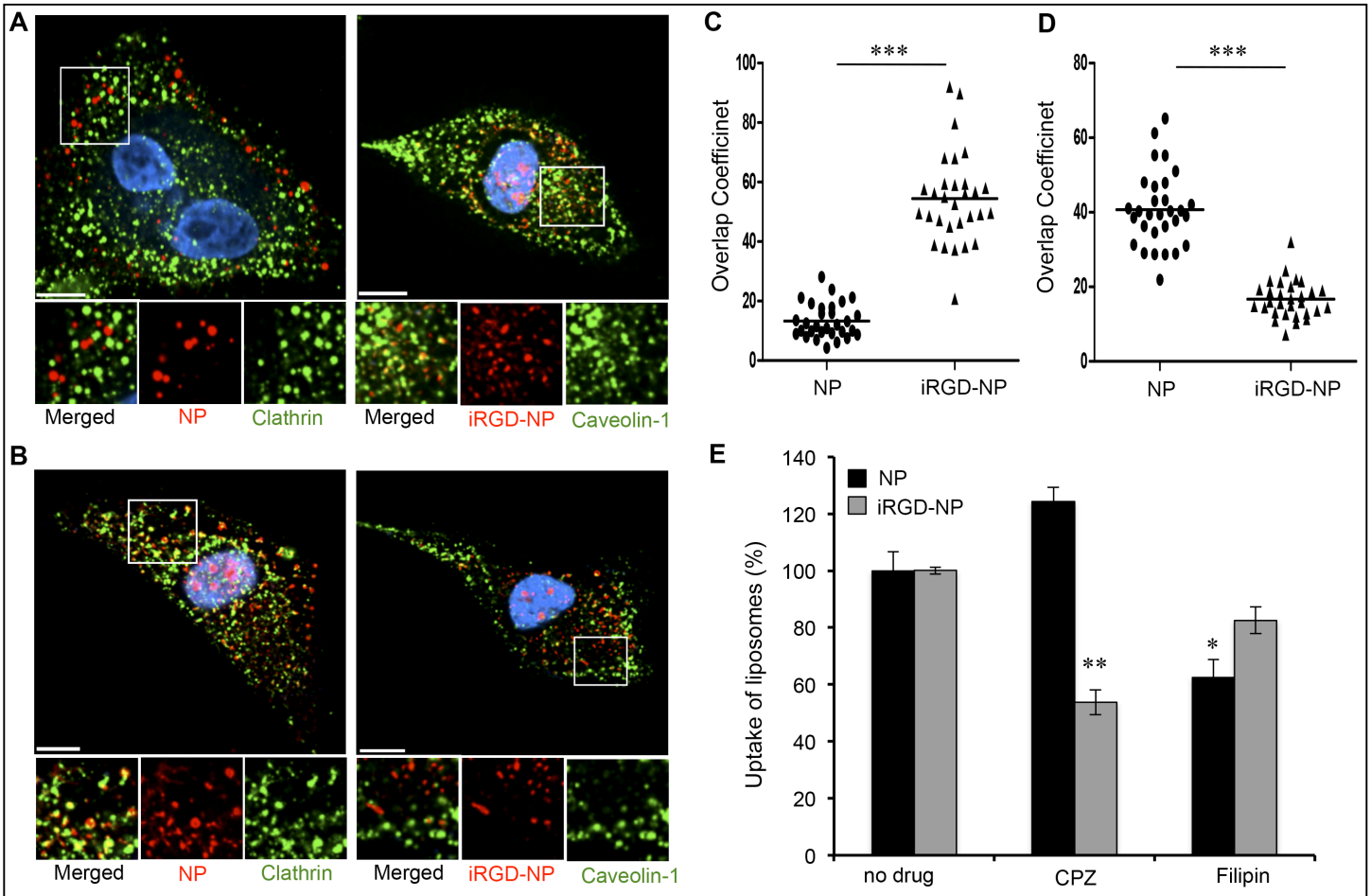


Figure 2: Clathrin-mediated internalization of iRGD-NPs and caveolin-dependent endocytosis of NPs. (A, B) HeLa cells were incubated with DiD-labeled NP nanoparticles (red, A) or DiD-labeled iRGD-NPs particles (red, B) for 30 min at 4°C to synchronize internalization. The cells were then incubated at 37°C for 15 min, fixed, permeabilized, and immunostained with anti-clathrin (green) or anti-caveolin-1 antibody (green). The nucleus of cells was counterstained with DAPI. Scale bar represents 10 μm. (C, D) Quantification of NP and iRGD-NP particles colocalized with clathrin (C) or caveolin-1 signals (D) after 15 min of incubation. Overlap coefficients were calculated using Manders' overlap coefficients by viewing more than 30 cells of each sample using the Nikon NIS-Elements software. Error bars represent the standard deviation of the mean from analysis of multiple images (***: $P < 0.005$). (E) Inhibition of clathrin-dependent endocytosis by chlorpromazine (CPZ, 25 μg/ml) and caveolin-dependent internalization by Filipin (10 μg/ml). The uptake of DiD-labeled NP and DiD-labeled iRGD-NP nanoparticles was determined by measuring DiD fluorescence via flow cytometry. Error bars represent the standard deviation of the mean from triplicate experiments (* $P < 0.05$, ** $P < 0.01$).

caveolin-dependent internalization (Rothberg, Heuser et al. 1992; Neufeld, Cooney et al. 1996). As shown in Figure 2E, CPZ (10 μg/ml) significantly decreased the uptake of iRGD-NPs in HeLa cells, while no significant inhibitory effect on their uptake was observed when cells were pretreated with Filipin (10 μg/ml). However, pretreatment of cells with Filipin remarkably decreased the uptake of unconjugated nanoparticles ($P < 0.01$), whereas no inhibitory effect on their uptake was observed in CPZ-pretreated cells. Results from the inhibition assay further confirmed that iRGD-NP endocytosis is mediated by the clathrin-dependent pathway, while unconjugated particles enter cells via caveolin-dependent endocytosis.

Once inside the cells, the intracellular fate of the endosomal contents has been considered as an important determinant of successful drug delivery (Bareford and Swaan 2007). It was also proposed that nanoparticles might transport to the early endosomes in a GTPase Rb5-dependent manner and also proceed

through the conventional endocytic pathway (endosomes/lysosomes) (Carlsson, Roth et al. 1988; Luzio, Brake et al. 1990; Christoforidis, McBride et al. 1999), probably resulting in enzymatic destruction of lipid membrane for drug release in lysosomes (Bareford and Swaan 2007). To further investigate the subsequent intracellular fate of iRGD-NPs, DiD-labeled iRGD-NPs were evaluated for their colocalization with the early endosome (EEA-1) (Pelkmans, Kartenbeck et al. 2001) and lysosome (Lamp-1) (Carlsson, Roth et al. 1988) markers at different incubation times at 37°C. As shown in Figure 3A, most iRGD-NPs were found in the $EEA1^+$ early endosomes after incubation of 30 min, validating the involvement of early endosomes in the intracellular fate of targeted nanoparticles. In addition, after 2h incubation, a significant colocalization of iRGD-NPs with lysosomes was observed, suggesting that iRGD-NPs may transport to early endosomes and further travel to lysosomes for possible release of drug from liposomes and endocytic compartments to cytosol. When taken together, the results showed that iRGD-NPs enter tumor cells via clathrin-dependent and receptor-mediated endocytosis, followed by transport through early endosomes and lysosomes.

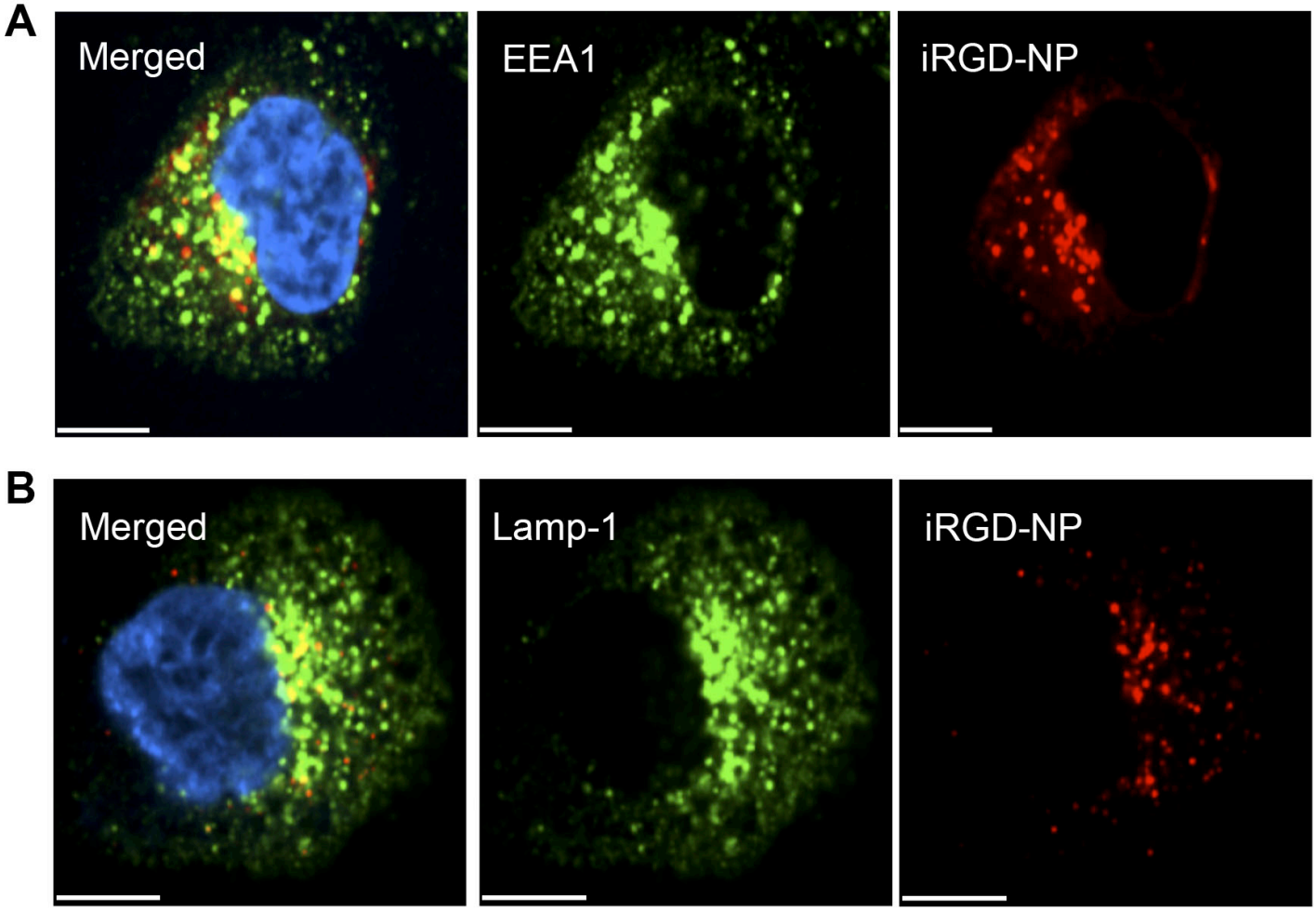


Figure 3: Involvement of early endosomes and lysosomes in the intracellular trafficking of iRGD-NPs. HeLa cells were incubated with DiD-labeled iRGD-NP nanoparticles (red) for 30 min at 4°C to synchronize internalization. The cells were then incubated at 37°C for 45 min and immunostained with anti-EEA1 antibody (green, A), or for 2 h and immunostained with anti-Lamp1 antibody (green, B). The nucleus of cells was counterstained with DAPI. Scale bar represents 10 μm.

**Task 5&6: Evaluating *in vivo* distribution and pharmacokinetics of nanocapsules**

For these tasks, we report our progress on utilizing positron emission tomography (PET) imaging to study in vivo biodistribution and pharmacokinetics of nanoparticles. We will still use the liposomal nanoparticles as the model system for testing the assays. For radiolabeling nanoparticles, amine-terminated PEG-SH was used for PEGylation of nanoparticles (UL and CML; UL: unilamellar nanoparticle; CML: crosslinked multilamellar

nanoparticle), while DSPE-PEG-$NH_2$ was used for PEGylation of DLLs (Doxil-like nanoparticle), in order to introduce amine groups onto liposomes for further reaction. Unless noted otherwise, all chemicals were

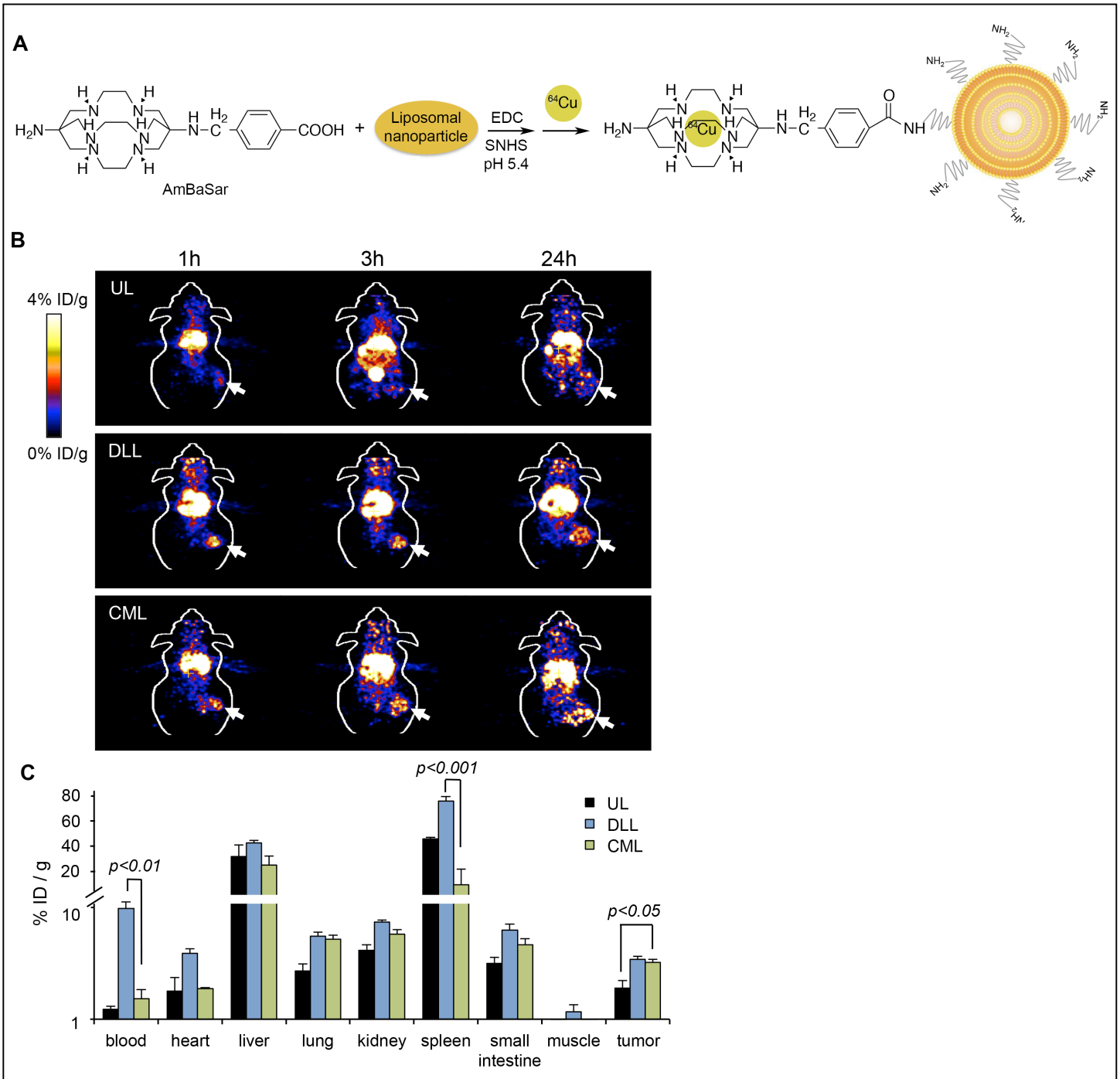


Figure 4: Biodistribution of drug carriers and accumulation of Dox in tumors. (A) Preparation of $^{64}$Cu-AmBaSar-labeled liposomes. (B) *In vivo* PET images of C57/BL6 mice bearing B16 tumors at 1, 3, and 24 h post-injection of $^{64}$Cu-AmBaSar-labeled UL, DLL, or CML. (C) Biodistribution of liposomes in different tissues at 24 h after injection with $^{64}$Cu-AmBaSar-labeled UL, DLL, or CML shown as percentage of injection dose per g of tissues (% ID/g).

analytic grade from Sigma-Aldrich (St. Louis, MO). $^{64}$Cu was produced using the $^{64}$Ni(p,n)$^{64}$Cu nuclear reaction and supplied in high specific activity as $^{64}CuCl_2$ in 0.1 N HCl. The bifunctional chelator AmBaSar was synthesized as reported (Cai, Li et al. 2010). AmBaSar was activated by EDC and SNHS. Typically, 5 mg of AmBaSar (11.1 μmol) in 100 μL water and 1.9 mg of EDC (10 μmol) in 100 μL water were mixed together, and 0.1 N NaOH (150 μL) was added to adjust the pH to 4.0. SNHS (1.9 mg, 8.8 μmol) was then added to the stirring mixture on ice-bath, and 0.1 N NaOH was added to finalize the pH to 4.0. The reaction remained at 4 °C for 30 min. The theoretical concentration of active ester AmBaSar-OSSu was calculated to be 8.8 μmol. Then, 5–20 times AmBaSar-OSSu (based on molar ratios) were loaded to the liposomes of interest. The pH

was adjusted to 8.5 using borate buffer (1M, pH 8.5). The reaction remained at 4 °C overnight, after which the size-exclusion PD-10 column was employed to afford the AmBaSar-conjugated liposomes in PBS buffer. AmBaSar-liposome was labeled with $^{64}$Cu by addition of 1–5 mCi of $^{64}$Cu (50–100 μg AmBaSar-liposome per mCi $^{64}$Cu) in 0.1 N phosphate buffer (pH 7.5), followed by 45 min incubation at 40 °C. $^{64}$Cu-AmBaSar-liposome was purified on a size exclusion PD-10 column using PBS as the elution solvent. Positron emission tomography (PET) imaging of the mice was performed using a microPET R4 rodent model scanner (Concorde Microsystems, Knoxville, TN). The B16-F10 tumor-bearing C57/BL6 mice were imaged in the prone position in the microPET scanner. The mice were injected with approximately 100 μCi $^{64}$Cu-AmBaSar-liposome via the tail vein. For imaging, the mice were anaesthetized with 2% isoflurane and placed near the center of the field of view (FOV), where the highest resolution and sensitivity are obtained. Static scans were obtained at 1, 3, and 24h post-injection. The images were reconstructed by a two-dimensional ordered subsets expectation maximum (2D-OSEM) algorithm. Time activity curves (TAC) of selected tissues were obtained by drawing regions of interest (ROI) over the tissue area. The counts per pixel/min obtained from the ROI were converted to counts per ml/min by using a calibration constant obtained from scanning a cylinder phantom in the microPET scanner. The ROI counts per ml/min were converted to counts per g/min, assuming a tissue density of 1 g/ml, and divided by the injected dose to obtain an image based on ROI-derived percent injected dose of $^{64}$Cu tracer retained per gram (%ID/g). For biodistribution, animals were sacrificed 24h post-injection; tissues and organs of interest were harvested and weighed. Radioactivity in each organ was measured using a gamma counter, and radioactivity uptake was expressed as percent injected dose per gram (%ID/g). Mean uptake (%ID/g) for each group of animals was calculated.

As shown in Figure 4B, the PET images were obtained at several time points (1, 3, 24 h) after intravenous injection of $^{64}$Cu-AmBaSar-labeled ULs, DLLs, or CMLs. After 1 h of administration, radioactivity was present mainly in well-perfused organs, and accumulation in tumors was detected in DLLs and CMLs compared with ULs. Furthermore, the accumulation of DLLs and CMLs in tumors significantly increased after 3 and 24 h of injection, whereas accumulation of ULs in the bladder was observed after 3 h of administration as a consequence of rapid degradation. In addition, the tumors and tissues of interest were then excised at 24 h post-injection and weighed, and accumulation levels of particles in the tumors and tissues were determined by measuring radioactivity (Figure 4C). This biodistribution assay revealed significantly higher accumulation of CMLs in tumors than that of ULs with the same lipid composition, suggesting that CMLs with improved vesicle stability could indeed enhance accumulation of drug carriers at the tumor site.

## KEY RESEARCH ACCOMPLISHMENTS

1) We have successfully demonstrated that iRGD peptides can facilitate binding and cellular uptake of nanoparticles.

2) Such targeted nanoparticles entered cells via the clathrin-mediated pathway, followed by endosome-lysosome transport.

3) As demonstrated in the model system, $^{64}$Cu-based labeling method can be used to study biodistribution and pharmacokinetics of nanocapsules.

## REPORTABLE OUTCOMES

**Publications*:***
The results above have been submitted for publication in *Nano Today*

Zhao, M., Hu, B., Gu, Z., Joo, K., Wang, P., Tang, Y. “Degradable Polymeric Nanocapsule for Efficient Intracellular Delivery of a High Molecular Weight Tumor-Selective Protein Complex.” *Nano Today.* **2013**, 8, 11-20.

## CONCLUSION

We were able to show that iRGD peptide could be conjugated into nano-size particles. Nanoparticles bearing iRGD could facilitate the binding and cellular uptake of drug-loaded nanoparticles. Imaging studies revealed that iRGD-conjugated nanoparticles was taken up by cells through the clathrin-mediated pathway, followed by endosome-lysosome transport. In addition, we were able to demonstrate that the biofunctional chelator AmBaSar could be used in the $^{64}$Cu labeling of nanoparticles and the positron emission tomography-based images of particle distribution could be obtained at several time points after intravenous administration of nanoparticles. Our data support the further experiment to use iRGD for targeting nanocapsules and to use PET imaging for investigating bioditribution of nanocapsule in vivo.

## REFERENCES


Atkins, J. H. and L. J. Gershell (2002). "Selective anticancer drugs." Nat Rev Drug Discov **1**(7): 491-492.

Backendorf, C., A. E. Visser, et al. (2008). "Apoptin: therapeutic potential of an early sensor of carcinogenic transformation." Annu Rev Pharmacol Toxicol **48**: 143-169.

Bareford, L. M. and P. W. Swaan (2007). "Endocytic mechanisms for targeted drug delivery." Adv. Drug Deliv. Rev. **59**: 748-758.

Brown, C. J., S. Lain, et al. (2009). "Awakening guardian angels: drugging the p53 pathway." Nat Rev Cancer **9**(12): 862-873.

Cai, H., Z. Li, et al. (2010). "An improved synthesis and biological evaluation of a new cage-like bifunctional chelator, 4-((8-amino-3,6,10,13,16,19-hexaazabicyclo[6.6.6]icosane-1-ylamino)methyl) benzoic acid, for 64Cu radiopharmaceuticals." Nucl Med Biol **37**(1): 57-65.

Carlsson, S. R., J. Roth, et al. (1988). "Isolation and Characterization of Human Lysosomal Membrane-Glycoproteins, H-Lamp-1 and H-Lamp-2 - Major Sialoglycoproteins Carrying Polylactosaminoglycan." J. Biol. Chem. **263**: 18911-18919.

Christoforidis, S., H. M. McBride, et al. (1999). "The Rab5 Effector Eea1 is a Core Component of Endosome Docking." Nature **397**: 621-625.

Conner, S. D. and S. L. Schmid (2003). "Regulated portals of entry into the cell." Nature(422): 37-44.

Cotter, T. G. (2009). "Apoptosis and cancer: the genesis of a research field." Nat Rev Cancer **9**(7): 501-507.

Danen-Van Oorschot, A. A., D. F. Fischer, et al. (1997). "Apoptin induces apoptosis in human transformed and malignant cells but not in normal cells." Proc Natl Acad Sci U S A **94**(11): 5843-5847.

Danen-Van Oorschot, A. A., Y. H. Zhang, et al. (2003). "Importance of nuclear localization of apoptin for tumor-specific induction of apoptosis." J Biol Chem **278**(30): 27729-27736.

Dobson, P. D. and D. B. Kell (2008). "Carrier-mediated Cellular Uptake of Pharmaceutical Drugs: an Exception or the Rule?" Nat. Rev. Drug Discov. **7**: 205-220.

Evan, G. I. and K. H. Vousden (2001). "Proliferation, cell cycle and apoptosis in cancer." Nature **411**(6835): 342-348.

Feron, O. (2010). "Tumor-penetrating peptides: a shift from magic bullets to magic guns." Sci Transl Med **2**.

Gibbs, J. B. (2000). "Mechanism-based target identification and drug discovery in cancer research." Science **287**(5460): 1969-1973.

Guelen, L., H. Paterson, et al. (2004). "TAT-apoptin is efficiently delivered and induces apoptosis in cancer cells." Oncogene **23**(5): 1153-1165.

Le Roy, C. and J. L. Wrana (2005). "Clathrin- and Non-clathrin-mediated Endocytic Regulation of Cell Signalling." Nat. Rev. Mol. Cell Biol. **6**: 112-126.

Leliveld, S. R., Y. H. Zhang, et al. (2003). "Apoptin induces tumor-specific apoptosis as a globular multimer." J Biol Chem **278**(11): 9042-9051.

Luzio, J. P., B. Brake, et al. (1990). "Identification, Sequencing and Expression of an Integral Membrane-Protein of the Trans-Golgi Network (Tgn38)." Biochem. J. **270**: 97-102.

Mitra, A., J. Mulhollan, et al. (2005). "Targeting tumor angiogenic vasculature using polymer–RGD conjugates." J Control Release **102**: 191-201.

Murphy, E. A., B. K. Majeti, et al. (2008). "Nanoparticle-mediated drug delivery to tumor vasculature suppresses metastasis." Proc Natl Acad Sci USA **105**: 9343-9348.

Neufeld, E. B., A. M. Cooney, et al. (1996). "Intracellular Trafficking of Cholesterol Monitored with a Cyclodextrin." J. Biol. Chem. **271**: 21604-21613.

Pelkmans, L. and A. Helenius (2002). "Endocytosis Via Caveolae." Traffic **3**: 311-320.

Pelkmans, L., J. Kartenbeck, et al. (2001). "Caveolar Endocytosis of Simian Virus 40 Reveals a New Two-step Vesicular-transport Pathway to the ER." Nat. Cell Biol. **3**: 473-483.

Petros, R. A. and J. M. DeSimone (2010). "Strategies in the Design of Nanoparticles for Therapeutic Applications." Nat. Rev. Drug Discov. **9**: 615-627.

Reed, J. C. (2003). "Apoptosis-targeted therapies for cancer." Cancer Cell **3**(1): 17-22.

Rothberg, K. G., J. E. Heuser, et al. (1992). "Caveolin, a Protein-Component of Caveolae Membrane Coats." Cell **68**: 673-682.

Sugahara, K. N., T. Teesalu, et al. (2009). "Tissue-penetrating delivery of compounds and nanoparticles into tumors." Cancer Cell **16**: 510-520.

Wang, L. H., K. G. Rothberg, et al. (1993). "Mis-Assembly of Clathrin Lattices on Endosomes Reveals a Regulatory Switch for Coated Pit Formation." J. Cell Biol. **123**: 1107-1117.

Zhuang, S. M., A. Shvarts, et al. (1995). "Apoptin, a protein derived from chicken anemia virus, induces p53-independent apoptosis in human osteosarcoma cells." Cancer Res **55**(3): 486-489.

Jain, R., 1999. Transport of molecules, particles, and cells in solid tumors. Annu. Rev. Biomed. **1**, 241-263.

Sugahara, K.N., Teesalu, T., Karmali, P.P., Kotamraju, V.R., Agemy, L., Greenwald, D.R., Ruoslahti, E., 2010. Coadministration of a Tumor-Penetrating Peptide Enhances the Efficacy of Cancer Drugs. Science **328**, 1031-1035.